

# NJC

Accepted Manuscript



This article can be cited before page numbers have been issued, to do this please use: Z. Lu, W. Fan, Y. Lu, C. Fan, H. Zhao, K. Guo, W. Chu and Y. Lu, *New J. Chem.*, 2018, DOI: 10.1039/C8NJ02197J.



This is an Accepted Manuscript, which has been through the Royal Society of Chemistry peer review process and has been accepted for publication.

Accepted Manuscripts are published online shortly after acceptance, before technical editing, formatting and proof reading. Using this free service, authors can make their results available to the community, in citable form, before we publish the edited article. We will replace this Accepted Manuscript with the edited and formatted Advance Article as soon as it is available.

You can find more information about Accepted Manuscripts in the [author guidelines](#).

Please note that technical editing may introduce minor changes to the text and/or graphics, which may alter content. The journal's standard [Terms & Conditions](#) and the ethical guidelines, outlined in our [author and reviewer resource centre](#), still apply. In no event shall the Royal Society of Chemistry be held responsible for any errors or omissions in this Accepted Manuscript or any consequences arising from the use of any information it contains.



Journal Name

ARTICLE

## A Highly sensitive fluorescent probe for bioimaging Zinc Ion in Living Cells and Zebrafish Models

Zhengliang Lu,<sup>\*,a</sup> Wenlong Fan,<sup>a</sup> Yanan Lu,<sup>a</sup> Chunhua Fan,<sup>\*,a</sup> Huaiqing Zhao,<sup>a</sup> Kai Guo,<sup>a</sup> Wei Chu, Yizhong Lu<sup>\*,b</sup>

Received 00th January 20xx,  
Accepted 00th January 20xx

DOI: 10.1039/x0xx00000x

[www.rsc.org/](http://www.rsc.org/)

Zn<sup>2+</sup> plays fundamental roles in cellular metabolism and apoptosis, as well as neurotransmission. However, it is still challenging and meaningful how to fast detect Zn<sup>2+</sup> in biology. In this report, we rationally synthesized a simple off-on fluorescent probe for fast detection of Zn<sup>2+</sup> based on intramolecular charge transfer and chelation enhanced fluorescence. Addition of Zn<sup>2+</sup> into the probe induced a significant fluorescence enhancement with a bathochromic shift of 55 nm. Moreover, the probe demonstrated excellent sensitivity (detection limit = 0.072 μM) and outstanding selectivity toward Zn<sup>2+</sup> and ultra-fast response rate of two seconds. The recognition mechanism of the probe toward Zn<sup>2+</sup> was fully confirmed by HRMS and <sup>1</sup>H NMR spectra, as well as TDDFT calculations. Furthermore, the probe could rapidly light-up bioimaging Zn<sup>2+</sup> in living cells and zebrafish models with low cytotoxicity and good biocompatibility.

### 1. Introduction

It is well known that small-molecular fluorescent probes are now regarded as an excellent technique that can visualize biological substances in living cells or organs due to high temporal and spatial resolution, ease of sample preparation, good sensitivity and selectivity.<sup>1-4</sup> Zn<sup>2+</sup>, as one of most abundant microelements, has been attracting more or more interests in biology and pharmacy for decades due to its important roles in many physiological and pathological processes including gene transcription and expression, cell division and proliferation, brain activity.<sup>5-7</sup> For example, Zn<sup>2+</sup> can endogenously neuro-modulate glutamate transmission.<sup>8, 9</sup> Being an important structural cofactor and catalytic center of hundreds of zinc proteins and regulators of enzymes, the fluctuation of Zn<sup>2+</sup> concentration are tightly associated with severe risks of physical growth retardation and neurological disorders such as cerebral ischemia, diabetes, Alzheimer's disease, amyotrophic lateral sclerosis.<sup>10, 11</sup>

Since the pioneering work sensing Zn<sup>2+</sup> in living cells and organs from several excellent research groups,<sup>12, 13</sup> there have been numerous Zn<sup>2+</sup>-specific fluorescent probes reported as a donor-acceptor (D-A) system in recent years.<sup>14-16</sup> These probes showed excellent absorption/fluorescence spectra or color change due to the effective modulation of electron transfer processes including

photoinduced electron transfer (PET), intramolecular charge transfer (ICT),<sup>17, 18</sup> excited-state intramolecular proton,<sup>19-22</sup> fluorescence resonance energy transfer,<sup>23</sup> or chelation enhanced fluorescence (CHEF).<sup>24</sup> In this regard, rational combinations of signal groups such as rhodamine,<sup>25, 26</sup> peptide,<sup>27</sup> diazafluorene,<sup>28</sup> coumarin,<sup>29</sup> 4-amino-1,8-naphthalimide,<sup>30, 31</sup> quinoline,<sup>32-34</sup> dipyrrometheneboron difluoride,<sup>35, 36</sup> fluorescein<sup>37</sup> and others,<sup>38-42</sup> and recognition sites including di(2-pyridylmethyl)-amine,<sup>43-45</sup> and *N,N*-di-(2-picoly)-ethylenediamine<sup>46</sup> have been proved to be an effective design strategy. It has to be pointed out that many of them showing remarkable fluorescence response and/or color change were obtained by complicated synthetic procedures. Recently, several two-photon (TP) fluorescent probes toward Zn<sup>2+</sup> were reported showing fluorescence emission under the long wave light excitation.<sup>47</sup> For example, Liu's group developed a TP fluorescent probe as a quinoline derivative for monitoring intracellular free Zn<sup>2+</sup>. Tian's group reported a TP fluorescent probe for ratiometric bioimaging Zn<sup>2+</sup> in hippocampal tissue and zebrafish upon excitation at 800 nm.<sup>48</sup> With regard to the naphthalene fluorophore, Kim's group reported a TP probe for imaging zinc ion distributed in Golgi upon excitation at 750 nm.<sup>49</sup> Meng's group synthesized a TP fluorescent probe containing quinoline and DPA for ratiometric sensing mitochondrial Zn<sup>2+</sup>.<sup>50</sup> Unfortunately, most fluorescent probes toward Zn<sup>2+</sup> including TP ones still suffered the interference from Cu<sup>2+</sup>, Cd<sup>2+</sup> or Fe<sup>3+</sup>.<sup>51-54</sup> Therefore, the development of fluorescent probes with excellent selectivity and sensitivity is still challenging and demanding to rapidly monitor the homeostasis of biological zinc ion.

Inspired by these nice research results for sensing Zn<sup>2+</sup>, in this report, we developed a simple Zn<sup>2+</sup> fluorescent probe (**Sen-OH**) based on a Schiff-base derivative with high selectivity and sensitivity. **Sen-OH** was synthesized via a one-step condensation of 5-phenylsalicylaldehyde and 2-aminobenzohydrazide. As

<sup>a</sup> Key Laboratory of Interfacial Reaction & Sensing Analysis in Universities of Shandong, School of Chemistry and Chemical Engineering, University of Jinan, Jinan 250022, China. Email: [zhengliang.lu@yahoo.com](mailto:zhengliang.lu@yahoo.com); [chm\\_fanch@ujn.edu.cn](mailto:chm_fanch@ujn.edu.cn)

<sup>b</sup> School of Materials Science and Engineering, University of Jinan, Jinan 250022, China. Email: [mse\\_luvz@ujn.edu.cn](mailto:mse_luvz@ujn.edu.cn)

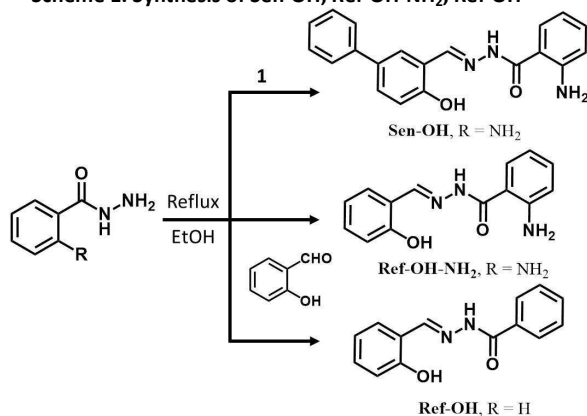
† Footnotes relating to the title and/or authors should appear here. Electronic Supplementary Information (ESI) available: [NMR spectra of the compounds, MS and chromatograms of the reaction systems, supplementary fluorescent spectra, cytotoxicity assay]. See DOI: 10.1039/x0xx00000x

## ARTICLE

## Journal Name

anticipated, addition of  $Zn^{2+}$  rapidly promoted a remarkable fluorescence enhancement with a low detection limit. Moreover, **Sen-OH** was low-cytotoxic and cell-permeable and successfully used for bioimaging  $Zn^{2+}$  in living cells and zebrafish models.

**Scheme 1. Synthesis of Sen-OH, Ref-OH-NH<sub>2</sub>, Ref-OH**



## 2. Experimental

### 2.1 Instruments and chemicals

All chemical reagents and solvents (analytical grade) were obtained commercially and used as received without further purification unless otherwise stated. <sup>1</sup>H NMR and <sup>13</sup>C NMR spectra were performed on a Bruker Advance DRX 400 spectrometer at 400 MHz/100 MHz. Mass spectra (ESI) were recorded on Bruker Waters-Q-TOF-Premier spectrometer. UV-Vis spectra were recorded on a TU-1901 spectrometer. Fluorescence spectra were conducted on a Hitachi F-4600 luminescence spectrophotometer with xenon lamp (Hitachi High-Technologies C., Japan). The pH value was measured by a Leici PHS-3C pH meter. The fluorescence images of cell and zebrafish were taken using a Leica confocal laser scanning microscope (Germany). 2-aminobenzohydrazide and **Ref-OH** were synthesized following a revised procedure.<sup>55</sup>

### 2.2 Synthesis of 5-phenylsalicylaldehyde (1)

5-phenylsalicylaldehyde was synthesized according to a modified procedure.<sup>56</sup> Dry paraformaldehyde (6.60 g, 220 mmol) was added to a mixture of 4-phenylphenol (2.72 g, 16 mmol), triethylamine (8.4 mL, 61 mmol) and anhydrous MgCl<sub>2</sub> (2.28 g, 24 mmol) in dry acetonitrile (50 mL). After refluxing for 6 h, the mixture was cooled to room temperature, acidified with 1M HCl, and extracted with ethyl acetate (3 × 20 mL). The combined organic layer was washed with water and dried over anhydrous MgSO<sub>4</sub>. After the solvent was removed under vacuum, the residue was purified by column chromatography to give 1.77 g of the title compound as a white solid (yield 65%). <sup>1</sup>H NMR (400 MHz, CDCl<sub>3</sub>) δ 11.01 (s, 1H), 9.98 (d, *J* = 0.6 Hz, 1H), 7.79 – 7.75 (m, 2H), 7.58 – 7.54 (m, 2H), 7.46 (dd, *J* = 8.5, 7.0 Hz, 2H), 7.39 – 7.34 (m, 1H), 7.08 (dd, *J* = 8.3, 0.7 Hz, 1H). <sup>13</sup>C NMR (100 MHz, CDCl<sub>3</sub>) δ 196.67, 160.97, 139.34, 135.77, 133.34, 131.88, 128.99, 127.40, 126.60, 120.71, 118.14. HRMS (ESI) calc. for [C<sub>13</sub>H<sub>10</sub>O<sub>2</sub>-H]<sup>-</sup>, 197.0603; found, 197.0601.

### 2.3 Synthesis of Sen-OH

The mixture of 5-phenylsalicylaldehyde (0.20 g, 1 mmol) and 2-aminobenzohydrazide (0.15 g, 1 mmol) in 20 mL of ethanol was refluxing overnight under stirring. After the precipitate was formed, the solvent was removed by a rotary evaporator. The pure title compound was obtained by recrystallization from ethanol as a yellow solid in 60% yield. <sup>1</sup>H NMR (400 MHz, Acetone-*d*<sub>6</sub>) δ 11.89 (s, 1H), 11.23 (s, 1H), 8.67 (s, 1H), 7.70 – 7.62 (m, 5H), 7.45 (t, *J* = 7.7 Hz, 2H), 7.37 – 7.30 (m, 1H), 7.25 (ddd, *J* = 8.4, 7.0, 1.5 Hz, 1H), 7.07 (d, *J* = 8.4 Hz, 1H), 6.86 (dd, *J* = 8.4, 1.1 Hz, 1H), 6.61 (ddd, *J* = 8.1, 7.1, 1.2 Hz, 1H), 6.39 (s, 2H). <sup>13</sup>C NMR (101 MHz, DMSO-*d*<sub>6</sub>) δ 165.04, 157.06, 150.31, 147.42, 139.43, 132.56, 131.38, 129.36, 128.84, 128.29, 127.53, 126.79, 126.13, 119.05, 117.00, 116.50, 114.59, 112.41. HRMS (ESI) calc. for [C<sub>20</sub>H<sub>17</sub>N<sub>3</sub>O<sub>2</sub>-H]<sup>-</sup>, 330.12425; found, 330.12476.

### 2.4 Synthesis of Ref-OH-NH<sub>2</sub>

The reference compound **Ref-OH-NH<sub>2</sub>** was prepared using salicylaldehyde following the same procedure as **Sen-OH** in 73% yield. <sup>1</sup>H NMR (400 MHz, Acetone-*d*<sub>6</sub>) δ 11.67 (s, 1H), 10.15 (s, 1H), 8.45 (s, 1H), 7.90 (dd, *J* = 7.8, 1.5 Hz, 1H), 7.37 (dd, *J* = 7.7, 1.7 Hz, 1H), 7.30 (m, 2H), 7.18 – 7.09 (m, 1H), 7.04 (dd, *J* = 7.8, 1.6 Hz, 1H), 6.99 (dd, *J* = 8.1, 1.1 Hz, 1H), 6.94 – 6.85 (m, 1H), 6.83 – 6.77 (m, 1H), 6.71 (td, *J* = 7.5, 1.1 Hz, 1H). <sup>13</sup>C NMR (100 MHz, DMSO-*d*<sub>6</sub>) δ 160.30, 157.60, 154.74, 149.56, 146.38, 134.27, 131.63, 130.48, 129.91, 128.11, 125.97, 124.13, 119.25, 119.03, 118.34, 117.65, 116.59, 115.84, 114.90, 113.17. HRMS (ESI) calc. for [C<sub>14</sub>H<sub>13</sub>N<sub>3</sub>O<sub>2</sub>-H]<sup>-</sup>, 254.0930; found, 254.0932.

### 2.5 Cell culture and fluorescence imaging

HeLa cells were grown in Dulbecco's Modified Eagle Medium (DMEM) supplemented with 10% fetal bovine serum, 1% antibiotics at 37°C in a 95% humidity atmosphere containing 5% CO<sub>2</sub>. After washing with Dulbecco's phosphate-buffered saline (DPBS) twice, HeLa cells were plated on a flatbottom 96-well plate in 100 μL of culture medium and incubated in 5% CO<sub>2</sub> at 37°C and adhered for 24 h. The cells were washed three times with PBS before further experiments. The viability was performed by a standard MTT method after the 24 h incubation of the cells with the probe at different concentrations. Two groups were set for bioimaging  $Zn^{2+}$  in living cells. In the control group, the cells were imaged after the cells were treated only with the probe for 30 min. In the experimental group, the images were taken after the above **Sen-OH**-pretreated cells were further incubated with  $Zn^{2+}$  for 30 min more.

### 2.6 In Vivo Imaging of Zebrafish.

Two-day old zebrafish were obtained from commercial suppliers. In the control group, the zebrafish were incubated only with the probe (5 μM) for 30 min and then washed three times with PBS buffer. In the experimental group, the zebrafish pretreated with **Sen-OH** (5 μM) for 30 min were further incubated with  $Zn^{2+}$  (100 μM). The images of zebrafish were taken on a confocal microscope excited at 405 nm.

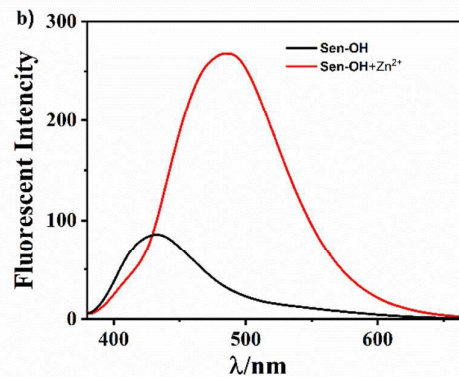
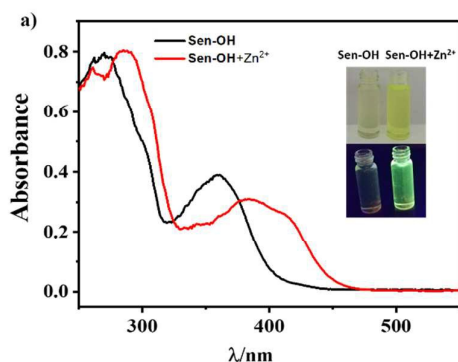
## 3. Results and discussion

### 3.1 Synthesis

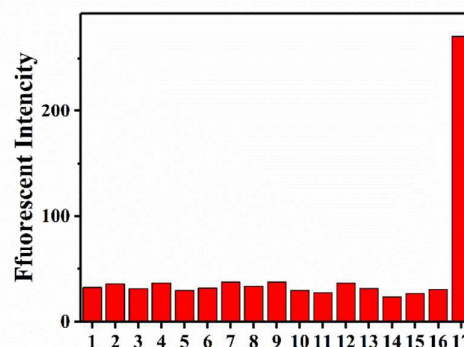
It is well known that many reported probes for  $\text{Zn}^{2+}$  were designed based on its strong affinity. This kind of probe usually holds a suitable cage to accommodate  $\text{Zn}^{2+}$ . With this thought, a simple Schiff-base probe was easily developed by a one-step condensation of 2-aminobenzohydrazide and 5-phenylsalicylaldehyde in good yield. In order to elucidate its characteristic, two reference compounds were synthesized following the similar procedure as **Sen-OH**. All compounds were characterized by  $^1\text{H}$  NMR,  $^{13}\text{C}$  NMR and ESI-MS analysis (SI, Figures S1-S5).

### 3.2 Fluorescence and absorption spectroscopic studies of **Sen-OH** toward $\text{Zn}^{2+}$

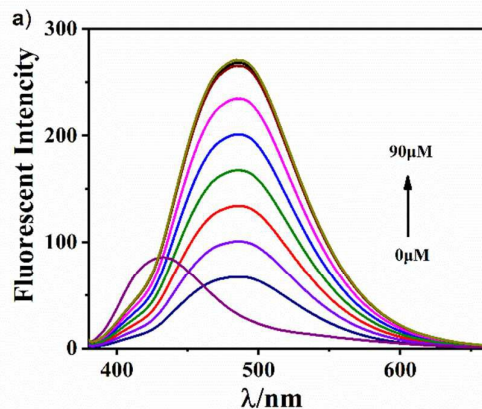
With the probe in hand, we first determined the feasibility of **Sen-OH** sensing  $\text{Zn}^{2+}$  by UV-visible and fluorescence spectra in  $\text{CH}_3\text{CN}$  aqueous solution (3:7, v/v, HEPES 20 mM, pH 7.4). As shown in Figure 1a, the UV-vis spectra of free **Sen-OH** (10  $\mu\text{M}$ ) exhibited an absorption band at 360 nm, which moved to a broad band at around 400 nm upon addition of 10 equiv. of  $\text{Zn}^{2+}$ . Additionally, an obvious color change from colorless to green was observed under 365 nm UV light (inset of Figure 1a). Free **Sen-OH** emitted weak fluorescence at 430 nm excited at 365 nm. Addition of  $\text{Zn}^{2+}$  led to disappearance of this emission and simultaneously formation of fluorescence at 485 nm (Figure 1b). After these initiation, the competition experiments of **Sen-OH** toward other common metal ions (70  $\mu\text{M}$ ) in  $\text{CH}_3\text{CN}$  aqueous solution (3:7, v/v, HEPES 20 mM, pH 7.4) were performed (Figure 2). As expected, there were no obvious fluorescence response even addition of 10 equiv. of competing metal ions such as  $\text{Mg}^{2+}$ ,  $\text{Al}^{3+}$ ,  $\text{Ag}^+$ ,  $\text{Ba}^{2+}$ ,  $\text{Ca}^{2+}$ ,  $\text{Cr}^{3+}$ ,  $\text{Cu}^{2+}$ ,  $\text{Fe}^{3+}$ ,  $\text{Hg}^{2+}$ ,  $\text{K}^+$ ,  $\text{Li}^+$ ,  $\text{Mn}^{2+}$ ,  $\text{Na}^+$ ,  $\text{Pb}^{2+}$ ,  $\text{Cd}^{2+}$  (Figure 2). However, only  $\text{Zn}^{2+}$  induced the distinct color and spectral change. Therefore, these attempts evidenced the outstanding selectivity of **Sen-OH** toward  $\text{Zn}^{2+}$  over other metal ions.



**Fig. 1** Absorption (a) and fluorescence (b) responses of **Sen-OH** (10  $\mu\text{M}$ ) in the absence and presence of  $\text{Zn}^{2+}$  (10 equiv) in  $\text{CH}_3\text{CN}$  aqueous solution (3:7, v/v, HEPES 20 mM, pH 7.4). The measurements were performed after the addition of  $\text{Zn}^{2+}$  for 10 min. Inset: photo graphs of **Sen-OH** (left) and **Sen-OH-Zn $^{2+}$**  (right) under natural light or an ultraviolet light.



**Fig. 2** Fluorescence responses of **Sen-OH** (10  $\mu\text{M}$ ) toward common competing metal ions (10 equiv.) in  $\text{CH}_3\text{CN}$  aqueous solution (3:7, v/v, HEPES 20 mM, pH 7.4). 1, Blank; 2,  $\text{Mg}^{2+}$ ; 3,  $\text{Al}^{3+}$ ; 4,  $\text{Ag}^+$ ; 5,  $\text{Cd}^{2+}$ ; 6,  $\text{Ba}^{2+}$ ; 7,  $\text{Ca}^{2+}$ ; 8,  $\text{Cr}^{3+}$ ; 9,  $\text{Cu}^{2+}$ ; 10,  $\text{Fe}^{3+}$ ; 11,  $\text{Hg}^{2+}$ ; 12,  $\text{K}^+$ ; 13,  $\text{Li}^+$ ; 14,  $\text{Mn}^{2+}$ ; 15,  $\text{Na}^+$ ; 16,  $\text{Pb}^{2+}$ ; 17,  $\text{Zn}^{2+}$ . The measurements were performed after addition of metal ions for 10 min. Excitation: 360 nm.



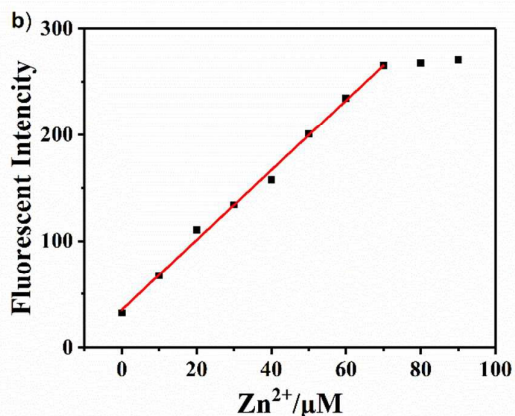


**Fig. 3** (a) Fluorescence spectra of **Sen-OH** (10  $\mu\text{M}$ ) in the presence of increasing concentrations of  $\text{Zn}^{2+}$  (0, 10, 20, 30, 40, 50, 60, 70, 80, 90  $\mu\text{M}$ ) in  $\text{CH}_3\text{CN}$  aqueous solution (3:7, v/v, HEPES 20 mM, pH 7.4). (b) Calibration curve of the fluorescence intensities ( $I_{485}$ ) versus the concentration of  $\text{Zn}^{2+}$ . Excitation: 360 nm. The measurements were performed after the addition of  $\text{Zn}^{2+}$  for 10 min.

Subsequently, the fluorescence titrations of **Sen-OH** toward  $\text{Zn}^{2+}$  in  $\text{CH}_3\text{CN}$  aqueous solution (3:7, v/v, HEPES 20 mM, pH 7.4) were performed to check the sensitivity of **Sen-OH**. As shown in Figure 3a, the free probe **Sen-OH** exhibited weak fluorescence at 430 nm upon excitation at 365 nm. Addition of  $\text{Zn}^{2+}$  reduced a new peak at 386 nm with a large bathochromic shift of 55 nm, which was assigned to **Sen-OH** binding  $\text{Zn}^{2+}$ . The fluorescence at 485 nm increased with gradually increasing concentration of  $\text{Zn}^{2+}$  and reached a maximum upon addition of 7 equiv. of  $\text{Zn}^{2+}$ . Furthermore, as shown in Figure 3b, the fluorescence intensity of **Sen-OH** at 485 nm was proportional to the gradually increasing concentration of  $\text{Zn}^{2+}$  ranging from 0 to 70  $\mu\text{M}$  with a  $R^2$  value of 0.996. The limit of detection (LOD) was evaluated to be 72 nM using the  $3\sigma/m$  equation, which is lower enough than 76  $\mu\text{M}$  of  $\text{Zn}^{2+}$  tolerance level in drinking water WHO recommends. These data suggested that **Sen-OH** sensitively responded toward  $\text{Zn}^{2+}$ . To proof the complexation stoichiometry of **Sen-OH**- $\text{Zn}^{2+}$ , a Job's plot of fluorescence intensity of **Sen-OH** against mole fractions of **Sen-OH** and  $\text{Zn}^{2+}$  was analyzed in  $\text{CH}_3\text{CN}$  aqueous (3:7, v/v, HEPES 20 mM, pH 7.4). As shown in Figure S6, The maximum emission intensity at a mole fraction of 0.3 indicated this 2:1 stoichiometry between **Sen-OH** and  $\text{Zn}^{2+}$ . Additionally, the reversibility of **Sen-OH** toward  $\text{Zn}^{2+}$  was confirmed by adding EDTA into **Sen-OH**- $\text{Zn}^{2+}$  in  $\text{CH}_3\text{CN}$ - $\text{H}_2\text{O}$  (Figure S7).

For on-site practical applications, photostability and response time are crucial parameters for fluorescent probes toward metal ions. Thus, we investigated the fluorescence changes of **Sen-OH** in presence of  $\text{Zn}^{2+}$  toward time. As showed in Figure S8, the fluorescence emission of **Sen-OH** sharply reached the maximum within two seconds after injection of  $\text{Zn}^{2+}$  in  $\text{CH}_3\text{CN}$  aqueous solution (3:7, v/v, HEPES 20 mM, pH 7.4), indicating the feasibility for real-time detection of  $\text{Zn}^{2+}$  in living systems with a high temporal resolution. There was no obvious changes of emission intensity observed over the subsequent 140 s. Additionally, The fluorescence

emission intensities of **Sen-OH** upon addition of  $\text{Zn}^{2+}$  at different concentrations (20, 60  $\mu\text{M}$ ) showed that the response time of **Sen-OH** is almost independent of the concentration of  $\text{Zn}^{2+}$ . Additionally, photostability was conducted in order to rule out the possibility of photobleaching interfering with detecting  $\text{Zn}^{2+}$ . The change of fluorescence intensity at 485 nm of **Sen-OH** (10  $\mu\text{M}$ ) in  $\text{CH}_3\text{CN}$ - $\text{H}_2\text{O}$  (v/v, 3:7, HEPES 20 mM, pH 7.4) were continuously monitored for every five minutes in absence and presence of UV light at 365 nm. As shown in Figure S9, we did not observe any significant change of fluorescence intensity even under UV irradiation of 365 nm for 30 minutes. These results implied that **Sen-OH** would rapidly and reliably sense  $\text{Zn}^{2+}$ .

### 3.3 Effect of pH.

In order to extend biological applications, the pH dependency on fluorescence intensity of **Sen-OH** was investigated in the absence and presence of  $\text{Zn}^{2+}$  at various pH value in  $\text{CH}_3\text{CN}$  aqueous solution. As shown in Figure S10, the fluorescence emission of **Sen-OH** sharply increased when  $\text{pH} > 8.5$ , which was attributed to deprotonation of hydroxyl group at high pH. Another reason could be that the basic condition accelerated the structural transformation from amide to imidic acid tautomer, which was also preferable for an effective conjugate system. However, addition of  $\text{Zn}^{2+}$  did not induce obvious fluorescence change when  $\text{pH} < 2.0$  probably because protonation of imine inhibited coordination of  $\text{Zn}^{2+}$  with **Sen-OH** under strongly acidic conditions. The fluorescence intensity of **Sen-OH** with  $\text{Zn}^{2+}$  remarkably increased under  $\text{pH} > 2.0$  and reached a plateau with no obvious changes after  $\text{pH} > 4.0$ , which was in good agreement with strong affinity toward  $\text{Zn}^{2+}$ . This wide pH range of 4-8.5 made **Sen-OH** suitable for  $\text{Zn}^{2+}$  detection under physiological conditions.

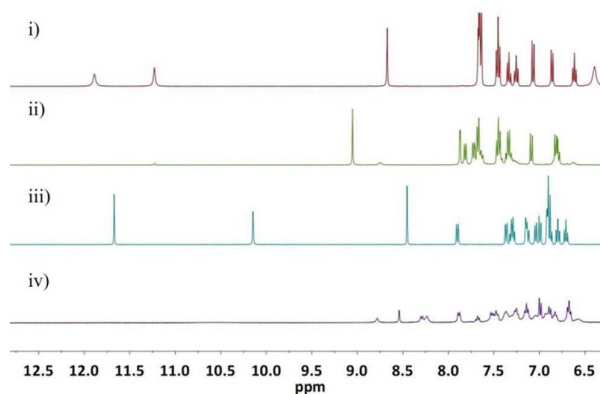


**Fig. 4** Partial  $^1\text{H}$  NMR spectra of (i) **Sen-OH** in acetone- $d_6$ , (ii) **Sen-OH**- $\text{Zn}^{2+}$  in acetone- $d_6$ , (iii) **Ref-OH** in acetone- $d_6$  and (iv) **Ref-OH**- $\text{Zn}^{2+}$  in acetone- $d_6$ .

### 3.4 Mechanism Studies

Most fluorescent probes for metal ion detection are designed based on its strong binding affinity.<sup>57-61</sup> Therefore, a suitable cage to accommodate metal ions is one of the most important structural characteristics of this kind of probes. The fluorescence intensity of probes for metal ions usually is reversible upon addition of strongly chelating reagents such as EDTA. In fact, the selectivity, sensitivity, or fluorescence intensity and emission wave length could be tuned

by a suitable substituent or conjugation.<sup>62</sup> Thus, we designed **Sen-OH** via a one-step condensation of 5-phenylsalicylaldehyde and 2-aminobenzohydrazide, which provided a three-atom cage composed of O, N and O from the hydroxyl, imine and imide, respectively. We imagined that addition of metal ions could modulate charge/electron processes in **Sen-OH** which finally emitted fluorescence. A feasible mechanism of **Sen-OH** detecting  $Zn^{2+}$  was demonstrated in Scheme S1. **Sen-OH** emitted weak fluorescence probably because of the PET process on. As anticipated, addition of  $Zn^{2+}$  into **Sen-OH** induced a remarkable fluorescence intensity enhancement. Concomitantly, the large bathochromic shift was also observed. Reasonably, these changes were attributed to the combination of ICT and CHEF induced by  $Zn^{2+}$  binding. The three-atom cage holding  $Zn^{2+}$  limited the free rotation and twist of **Sen-OH**, which led to the good rigidity and high coplanarity of the molecular assembly. The similar cage was confirmed to be much effective for  $Zn^{2+}$  selectivity by two or three-input logic gate designed by Yin or Glass's group.<sup>63,64</sup> Moreover, the structural transformation from amide to imidic acid tautomer happened in the presence of  $Zn^{2+}$ , being propitious to form an extended conjugate system. In order to more clearly elucidate the proposed mechanism, HRMS of **Sen-OH** were conducted in the absence and presence of  $Zn^{2+}$ . Besides a peak at  $m/z = 332.12476$  assigned to the free probe ( $[M+H]^+$ ): calcd 332.13941, Figure S11), Figure S11 demonstrated a new peak at  $m/z = 725.18491$ , which corresponded to **Sen-OH**- $Zn^{2+}$  ( $[2M+Zn^{2+}-H]^+$ ): calcd 725.18548). This complexation was fully consistent with the 2:1 stoichiometric ratio from the Job's plot.

Moreover,  $^1H$  NMR titrations of **Sen-OH** without or with  $Zn^{2+}$  in acetone- $d_6$  were carried out to evidence its strong binding ability to  $Zn^{2+}$  (Figure 4). Without  $Zn^{2+}$ , the probe **Sen-OH** in acetone- $d_6$  showed an amide proton peak at 11.89 ppm and a hydroxyl proton peak at 11.23 ppm (Figure 4i). As expected, both chemical shifts completely disappeared in the presence of  $Zn^{2+}$ , which indicated that the three-atom cage chelated  $Zn^{2+}$  and amide  $NH-C(=O)-$  transformed its imidic acid tautomer ( $-N=C(OH)-$ ) (Figure 4ii). This structural transformation enlarged the conjugate system, in which  $Zn^{2+}$ -binding could inhibit PET and concomitantly enable both ICT and CHEF. The complexation of **Sen-OH** and  $Zn^{2+}$  was further evidenced by the fact that the chemical shift of imine proton at 8.67 ppm downfield shifted to 9.05 ppm accompanied by considerable downfield shifts of aromatic protons.

In order to validate the significant contribution of the 5-phenyl and aniline group of **Sen-OH**, two reference compounds **Ref-OH** and **Ref-OH-NH<sub>2</sub>** were synthesized using salicylaldehyde and amino salicylaldehyde. As shown in Figure 4iii and iv, the vanishing of chemical shifts of amide proton at 11.67 ppm and phenolic proton at 10.15 ppm in  $^1H$  NMR spectrum of **Ref-OH** in the presence of  $Zn^{2+}$  confirmed the strong coordination ability of the three-atom cage to  $Zn^{2+}$ . A series of fluorescence spectra of **Ref-OH** and **Ref-OH-NH<sub>2</sub>** with or without  $Zn^{2+}$  were performed in  $CH_3CN$  aqueous solution (3:7, v/v, HEPES 20 mM, pH 7.4). As shown in Figure S12, **Ref-OH** showed a slight fluorescence enhancement. But **Ref-OH-NH<sub>2</sub>** demonstrated only a small red shift from 450 to 485 nm, which indicated that the amino group could act as an auxochrome. Such a group containing lone pair electrons can shift the maximum emission peak to the long wave range. Probably, in the presence of

$Zn^{2+}$ , the introduction of 5-phenyl as an hyperchromic group led to a remarkable emission enhancement at 485 nm by further enlarging the effective conjugated system of **Sen-OH**. All these data evidenced our speculation that the rational introduction of the phenyl and amino group to **Sen-OH** can modulate electron transfer process.

TDDFT calculations using Gaussian 09 program at the B3LYP/6-31G level were performed to illustrate the above feasible mechanism of **Sen-OH** sensing  $Zn^{2+}$ . The optimized structures of **Sen-OH** and the complex **Sen-OH**- $Zn^{2+}$  are shown in Figure 5. The HOMO mainly distributed in amino benzene moiety. However, the LUMO located on amide, imine and hydroxyl benzene groups other than the 5-phenyl group. The energy gap between HOMO and LUMO of free probe was 2.56 eV. In the probe- $Zn^{2+}$  (2:1) complex, the HOMO mainly distributed in the entire 5-phenylsalicylaldehyde moiety due to the presence of  $Zn^{2+}$ . The LUMO still located on amino benzene moiety from the other probe molecule of the complex. The lower energy gap of 1.61 eV in the complex corresponded to the red shift of fluorescence. These computational calculations supported our design concept, in which the substituent was allowed to endow **Sen-OH** with the promising properties.

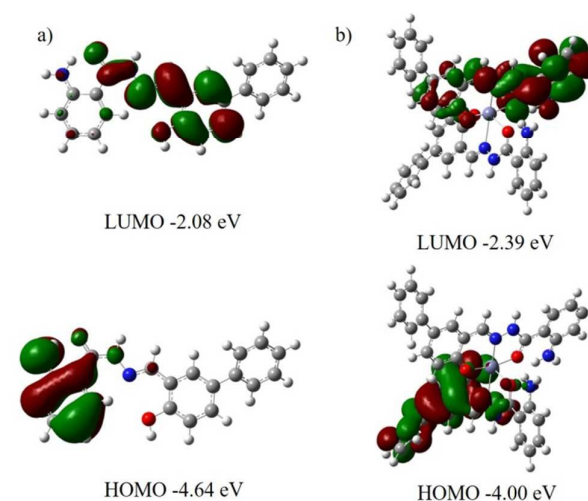
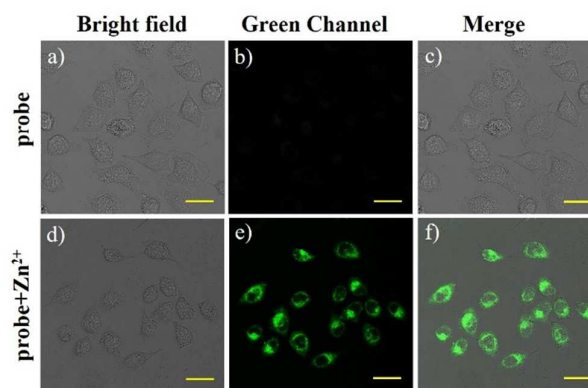


**Fig. 5** Optimized structures and frontier molecular orbitals of (a) **Sen-OH**, (b) **Sen-OH**: $Zn^{2+}$  (2:1). Calculations were performed at B3LYP/6-31G level.



## ARTICLE

## Journal Name

**Fig. 6** Confocal fluorescence images of living HeLa cells treated with **Sen-OH** in the absence and presence of  $Zn^{2+}$ . (a) Bright field image of HeLa cells with **Sen-OH**. (b) Image of (a). (c) Overlay of (a) and (b). (d) Bright field image of HeLa cells with **Sen-OH** and  $Zn^{2+}$ . (e) Image of (d). (f) Overlay of (d) and (e). The excitation wavelength is 405 nm and the emission was collected at 500-550 nm.

### 3.5 Imaging of $Zn^{2+}$ in Living Cells and zebrafish models.

Before we pursued more potential applications in biology, first, the cell cytotoxicity and biocompatibility of the probe were been examined by standard 3-(4,5-dimethylthiazol-2-yl)-2,5-diphenyltetrazolium bromide (MTT) assays. HeLa cells were incubated with different concentration probe **Sen-OH** (0, 5, 10, 15, 20  $\mu$ M) for 24 h. As shown in Figure S13, we observed that the cell maintained its high viability of 90% even the concentration of the probe was up to 15  $\mu$ M. Thus, the probe **Sen-OH** demonstrated the low cytotoxicity and good biocompatibility to living HeLa cell samples.

Inspired by the aforementioned sensing performance including high specificity, quantitative detection, high temporal resolution, low cytotoxicity and good biocompatibility, we next tested the feasibility of **Sen-OH** for bioimaging  $Zn^{2+}$  in living HeLa cells with a confocal laser scanning microscope (Leica, Germany). After HeLa cells were incubated with **Sen-OH** (5  $\mu$ M) for 10 min and washed three times with PBS buffer, as shown in Figure 6a-c, no obvious fluorescence no matter under bright field or green channel was observed upon excitation at 405 nm. As anticipated, when the cells pretreated with the probe (5  $\mu$ M) for 10 min were further incubated with  $Zn^{2+}$  for 10 min more, they emitted the remarkable green fluorescence (Figure 4e-f). These results indicated that **Sen-OH** could fast visualize intracellular  $Zn^{2+}$  in living cells with a good cell-penetrating ability.

Next, we tested the feasible application on bioimaging  $Zn^{2+}$  in living Zebrafish models. As show in Figure 7 a-c, first, 2-day-old zebrafish treated only with **Sen-OH** (5  $\mu$ M) for 10 min did not emit any fluorescence. However, there was the strong fluorescence when zebrafish was pretreated with the probe and then  $Zn^{2+}$  (Figure 7e-f). These results suggested that **Sen-OH** could be used for bioimaging  $Zn^{2+}$  in vivo.

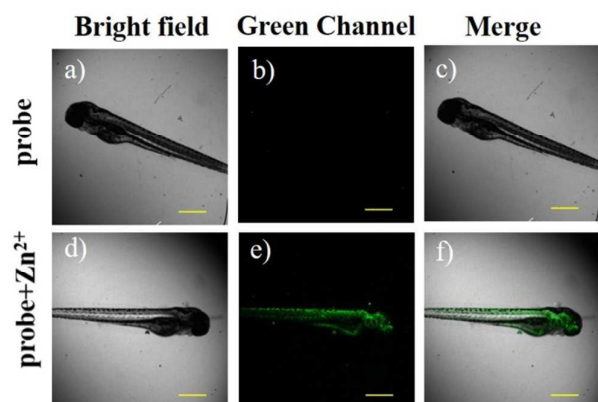


**Fig. 7** Confocal fluorescence images of living zebrafish treated with **Sen-OH** with or without  $Zn^{2+}$ . (a) Bright field image of zebrafish. (b) Green channel image of (a). (c) Overlay of (a) and (b). (d) Bright field image of zebrafish with **Sen-OH** and then  $Zn^{2+}$ . (e) Green channel image of (d). (f) Overlay of (d) and (e). The excitation wavelength is 405 nm and the emission was collected at 500-550 nm.

## 4. Conclusions

In summary, we have reported a simple off-on fluorescent probe for  $Zn^{2+}$  detection under physiological conditions. Addition of  $Zn^{2+}$  into the probe led to the strong green fluorescence emission in  $CH_3CN$  aqueous solution with a large red shift. This probe showed high selectivity and sensitivity to  $Zn^{2+}$  over other competing metal ions. The response time of less than 2 seconds made the probe suitable for further on-site applications. The  $Zn^{2+}$  recognition mechanism was fully supported by HRMS,  $^1H$  NMR titrations, as well as theoretical calculations. Furthermore, the probe was successfully applied for bioimaging  $Zn^{2+}$  in living HeLa cells and zebrafish models with excellent biocompatibility and low cell cytotoxicity.

## Acknowledgments

We thank for the supporting from Natural Science Foundation of China (grant No. 21101074), Shandong Provincial Natural Science Foundation of China (grant No. ZR2013BQ009 and ZR2016BL17), the Doctor's Foundation of University of Jinan (Grant No. XBS1320).

## Notes and References

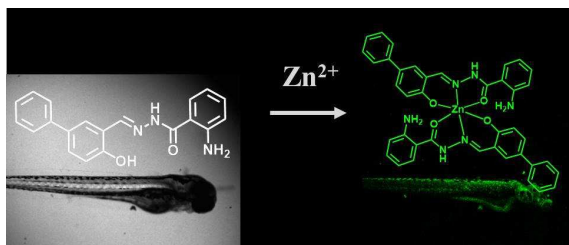
- B. A. Smith, W. J. Akers, W. M. Leevy, A. J. Lampkins, S. Xiao, W. Wolter, M. A. Suckow, S. Achilefu and B. D. Smith, *J. Am. Chem. Soc.*, 2010, **132**, 67-69.
- J. M. Berg and Y. Shi, *Science*, 1996, **271**, 1081-1085.
- Y. Tang, D. Lee, J. Wang, G. Li, J. Yu, W. Lin and J. Yoon, *Chem. Soc. Rev.*, 2015, **44**, 5003-5015.
- G. Sivaraman, M. Iniya, T. Anand, N. G. Kotla, O. Sunnapu, S. Singaravadiel, A. Gulyani and D. Chellappa, *Coord. Chem. Rev.*, 2018, **357**, 50-104.
- Z. Xu, J. Yoon and D. R. Spring, *Chem. Soc. Rev.*, 2010, **39**, 1996-2006.
- C. J. Frederickson, J.-Y. Koh and A. I. Bush, *Nat. Rev. Neurosci.*, 2005, **6**, 449-462.
- B. L. Vallee and K. H. Falchuk, *Physiol. Rev.*, 1993, **73**, 79-118.
- J. H. Weiss, S. L. Sensi and J. Y. Koh, *Trends Pharmacol. Sci.*, 2000, **21**, 395-401.
- B. K. Y. Bitanhirwe and M. G. Cunningham, *Synapse*, 2009, **63**, 1029-1049.
- A. I. Bush, *Trends Neurosci.*, 2003, **26**, 207-214.
- A. B. Chausmer, *J. Am. Coll. Nutr.*, 1998, **17**, 109-115.
- E. L. Que, D. W. Domaille and C. J. Chang, *Chem. Rev.*, 2008, **108**, 1517-1549.
- E. M. Nolan and S. J. Lippard, *Acc. Chem. Res.*, 2009,

- 42**, 193-203.
14. J. Li, C. Yin and F. Huo, *Dyes Pigm.*, 2016, **131**, 100-133.
  15. P. Jiang and Z. Guo, *Coord. Chem. Rev.*, 2004, **248**, 205-229.
  16. Y. Ding, Y. Tang, W. Zhu and Y. Xie, *Chem. Soc. Rev.*, 2015, **44**, 1101-1112.
  17. T. Wei, J. Wang, Y. Chen and Y. Han, *RSC Adv.*, 2015, **5**, 57141-57146.
  18. J. Wu, R. Sheng, W. Liu, P. Wang, H. Zhang and J. Ma, *Tetrahedron*, 2012, **68**, 5458-5463.
  19. J. E. Kwon, S. Lee, Y. You, K.-H. Baek, K. Ohkubo, J. Cho, S. Fukuzumi, I. Shin, S. Y. Park and W. Nam, *Inorg. Chem.*, 2012, **51**, 8760-8774.
  20. Y. Xu and Y. Pang, *Dalton Trans.*, 2011, **40**, 1503-1509.
  21. K. Zhang, S. Wu, D. Qu and L. Wang, *Tetrahedron Lett.*, 2016, **57**, 1133-1137.
  22. J. Nie, N. Li, Z. Ni, Y. Zhao and L. Zhang, *Tetrahedron Lett.*, 2017, **58**, 1980-1984.
  23. J.-F. Zhu, H. Yuan, W.-H. Chan and A. W. M. Lee, *Tetrahedron Lett.*, 2010, **51**, 3550-3554.
  24. K. Aich, S. Goswami, S. Das and C. D. Mukhopadhyay, *RSC Adv.*, 2015, **5**, 31189-31194.
  25. O. Sunnapu, N. G. Kotla, B. Maddiboyina, S. Singaravadivel and G. Sivaraman, *RSC Adv.*, 2016, **6**, 656-660.
  26. G. Sivaraman, T. Anand and D. Chellappa, *Analyst*, 2012, **137**, 5881-5884.
  27. G. Donadio, R. Di Martino, R. Oliva, L. Petraccone, P. Del Vecchio, B. Di Luccia, E. Ricca, R. Istitato, A. Di Donato and E. Notomista, *J. Mater. Chem. B*, 2016, **4**, 6979-6988.
  28. H. Li, S. J. Zhang, C. L. Gong, J. Z. Wang and F. Wang, *J. Fluoresc.*, 2016, **26**, 1555-1561.
  29. Z. Xu, X. Liu, J. Pan and D. R. Spring, *Chem. Commun.*, 2012, **48**, 4764-4766.
  30. J. H. Lee, J. H. Lee, S. H. Jung, T. K. Hyun, M. Feng, J.-Y. Kim, J.-H. Lee, H. Lee, J. S. Kim, C. Kang, K.-Y. Kwon and J. H. Jung, *Chem. Commun.*, 2015, **51**, 7463-7465.
  31. Y. Tang, J. Sun and B. Yin, *Anal. Chim. Acta*, 2016, **942**, 104-111.
  32. M. Akula, P. Z. El-Khoury, A. Nag and A. Bhattacharya, *RSC Adv.*, 2014, **4**, 25605-25608.
  33. G. J. Park, J. J. Lee, G. R. You, L. T. Nguyen, I. Noh and C. Kim, *Sens. Actuators, B*, 2016, **223**, 509-519.
  34. S. J. Rane, G. Sivaraman, A. M. Pushpalatha and S. Muthusubramanian, *Sens. Actuators, B*, 2018, **255**, 630-637.
  35. J.-R. Lin, C.-J. Chu, P. Venkatesan and S.-P. Wu, *Sens. Actuators, B*, 2015, **207**, 563-570.
  36. V. K. Gujuluva Gangatharan, K. Mookkandi Palsamy, S. Gandhi, A. Jamespandi, A. Kandasamy, T. Arunachalam, A. Shenmuganarayanan, S. Balasubramaniyam and R. Jegathalaprathaban, *Sens. Actuators, B*, 2018, **255**, 3235-3247.
  37. D. Li, L. Liu and W.-H. Li, *ACS Chem. Biol.*, 2015, **10**, 1054-1063.
  38. S. Y. Lee, S. Y. Kim, J. A. Kim and C. Kim, *J. Lumin.*, 2016, **179**, 602-609.
  39. Q. Jiang, Z. Guo, Y. Zhao, F. Wang and L. Mao, *Analyst*, 2015, **140**, 197-203.
  40. S. A. Ingale and F. Seela, *J. Org. Chem.*, 2012, **77**, 9352-9356.
  41. K. M. Vengaiyan, C. D. Britto, K. Sekar, G. Sivaraman and S. Singaravadivel, *Sens. Actuators, B*, 2016, **235**, 232-240.
  42. O. Sunnapu, N. G. Kotla, B. Maddiboyina, G. S. Asthana, J. Shanmugapriya, K. Sekar, S. Singaravadivel and G. Sivaraman, *Sens. Actuators, B*, 2017, **246**, 761-768.
  43. K. Hanaoka, K. Kikuchi, H. Kojima, Y. Urano and T. Nagano, *J. Am. Chem. Soc.*, 2004, **126**, 12470-12476.
  44. Z. Xu, K.-H. Baek, H. N. Kim, J. Cui, X. Qian, D. R. Spring, I. Shin and J. Yoon, *J. Am. Chem. Soc.*, 2010, **132**, 601-610.
  45. B. Tang, H. Huang, K. Xu, L. Tong, G. Yang, X. Liu and L. An, *Chem. Commun.*, 2006, 3609-3611.
  46. G. Masanta, C. S. Lim, H. J. Kim, J. H. Han, H. M. Kim and B. R. Cho, *J. Am. Chem. Soc.*, 2011, **133**, 5698-5700.
  47. H.-J. Lee, C.-W. Cho, H. Seo, S. Singha, Y. W. Jun, K.-H. Lee, Y. Jung, K.-T. Kim, S. Park, S. C. Bae and K. H. Ahn, *Chem. Commun.*, 2016, **52**, 124-127.
  48. W. Li, B. Fang, M. Jin and Y. Tian, *Anal. Chem.*, 2017, **89**, 2553-2560.
  49. H. Singh, H. W. Lee, C. H. Heo, J. W. Byun, A. R. Sarkar and H. M. Kim, *Chem. Commun.*, 2015, **51**, 12099-12102.
  50. P. Ning, J. Jiang, L. Li, S. Wang, H. Yu, Y. Feng, M. Zhu, B. Zhang, H. Yin, Q. Guo and X. Meng, *Biosens. Bioelectron.*, 2016, **77**, 921-927.
  51. W. Li, X. Tian, B. Huang, H. Li, X. Zhao, S. Gao, J. Zheng, X. Zhang, H. Zhou, Y. Tian and J. Wu, *Biosens. Bioelectron.*, 2016, **77**, 530-536.
  52. M.-Y. Jia, Y. Wang, Y. Liu, L.-Y. Niu and L. Feng, *Biosens. Bioelectron.*, 2016, **85**, 515-521.
  53. K. Wechakorn, K. Suksen, P. Piyachaturawat and P. Kongsaree, *Sens. Actuators, B*, 2016, **228**, 270-277.
  54. Y. Ikawa, M. Takeda, M. Suzuki, A. Osuka and H. Furuta, *Chem. Commun.*, 2010, **46**, 5689-5691.
  55. C. Yu, T. Wang, K. Xu, J. Zhao, M. Li, S. Weng and J. Zhang, *Dyes Pigm.*, 2013, **96**, 38-44.
  56. C. Fan, X. Huang, C. A. Black, X. Shen, J. Qi, Y. Yi, Z. Lu, Y. Nie and G. Sun, *RSC Adv.*, 2015, **5**, 70302-70308.
  57. S. Y. Ryu, M. Huh, Y. You and W. Nama, *Inorg. Chem.*, 2015, **54**, 9704-9714.
  58. V. V. S. Mummidiwarapu, S. Bandaru, D. S. Yarramala, K. Samanta, D. S. Mhatre and C. P. Rao, *Anal. Chem.*, 2015, **87**, 4988-4995.

## ARTICLE

Journal Name

59. L. Zhou, Q. Wang, X.-B. Zhang and W. Tan, *Anal. Chem.*, 2015, **87**, 4503-4507.
60. S. Zhu, J. Zhang, J. Janjanam, G. Vegesna, F.-T. Luo, A. Tiwari and H. Liu, *J. Mater. Chem. B*, 2013, **1**, 1722-1728.
61. K. P. Divya, S. Sreejith, P. Ashokkumar, Y. Kang, Q. Peng, S. K. Maji, Y. Tong, H. Yu, Y. Zhao, P. Ramamurthy and A. Ajayaghosh, *Chem. Sci.*, 2014, **5**, 3469-3474.
62. J. Shanmugapriya, K. Rajaguru, G. Sivaraman, S. Muthusubramanian and N. Bhuvanesh, *RSC Adv.*, 2016, **6**, 85838-85843.
63. C. Yin, F. Huo, N. P. Cooley, D. Spencer, K. Bartholomew, C. L. Barnes and T. E. Glass, *ACS Chem. Neurosci.*, 2017, **8**, 1159-1162.
64. K. S. Hettie, J. L. Klockow and T. E. Glass, *J. Am. Chem. Soc.*, 2014, **136**, 4877-4880.



A simple off-on fluorescent probe was prepared and successfully applied for bioimaging

$Zn^{2+}$  in living systems.